Received: 31 May 2019 | Revised: 14 August 2019 | Accepted: 14 September 2019

DOI: 10.1002/aic.16808

Check for updates

PROCESS SYSTEMS ENGINEERING

AIChE JOURNAL

Designing optimally-graded depth filter media using a novel multiscale method

Constantin Geerling[1] | Mehdi Azimian[2] | Andreas Wiegmann[2] | Heiko Briesen[1] | Michael Kuhn[1]

[1]Chair of Process Systems Engineering, Technical University of Munich, Munich, Germany

[2]Math2Market GmbH, Kaiserslautern, Germany

Correspondence
Michael Kuhn, Chair of Process Systems Engineering, Technical University of Munich, Gregor-Mendel Straße 4, 85354 Freising, Munich, Germany.
Email: michael.kuhn@tum.de

Abstract

Even though current manufacturing methods allow to build precisely-defined graded depth filter media, it remains unclear which local filtration properties are desirable. We, therefore, introduce a multiscale approach which links pore and continuum scale (PS and CS) to address this question. Based on data from PS simulations, local filtration performance, as described by the filter coefficient, is predicted on the CS by an optimal control solution and the obtained trajectory is translated back to the PS where it is validated. Two case studies are presented: a bidisperse fibrous medium and a granular depth filter composed of bidisperse particles. Both media are optimized to achieve a homogenous deposition of separated impurities along the filter depth. It is found that the presented method allows to reach this goal reasonably well in both cases. We claim that our method forms a good basis for further developments for which promising possibilities are highlighted.

KEYWORDS

depth filtration, filter media, graded media, optimization, process systems engineering

1 | INTRODUCTION

Depth filters are employed for various purposes, for the purification of liquids as well as the cleaning of gases. The general principle is also used in different industries, such as energy conversion, waste water treatment, beverage technology, and air conditioning.[1,2] All forms of depth filters are characterized by their phenomenological separation behavior, namely that the dispersed particles are captured within the filter medium, as contrasted to pure cake filtration where they are separated on top of the medium.[3-5] To achieve this depth-filtration behavior, filter pores are usually chosen significantly larger than the particles to be separated and, therefore, they are able to penetrate the medium.[4,6] However, it is important to mention that pure depth and cake filtration are idealized concepts seldomly encountered in practice, where, for example, depth filters often also show some cake formation on top of the medium.[7]

The present work is based on two previous studies conducted by separate research groups.[7,8] Both studies observed the lack of suitable design strategies for depth filters and made, coming from different directions, a very similar proposal to optimize filter design, namely the use of computationally determined graded structures. For these graded structures, a superior filter behavior in terms of pressure drop or filter life time, respectively, were observed. Azimian et al.[7] studied different designs of fibrous filters by pore-scale (PS) simulations and proposed a structure with an exponentially increasing fine fiber fraction from fluid inlet to outlet as a suitable setup. Kuhn et al.[8] presented a design method for depth filters using an optimal-control approach based on continuum models. In the present study, both research groups bring together their findings to develop a novel multiscale method for optimizing depth filter design. This approach combines the detailed physical insights from the PS with the computational efficiency and predictive power from the continuum scale (CS).

This is an open access article under the terms of the Creative Commons Attribution License, which permits use, distribution and reproduction in any medium, provided the original work is properly cited.
© 2019 The Authors. *AIChE Journal* published by Wiley Periodicals, Inc. on behalf of American Institute of Chemical Engineers.

In this multiscale approach, all necessary parameters for the continuum models are calculated from PS simulations. The parameterized continuum models are subsequently used for determining the optimal filter design. In a last step, these predictions are translated back to the PS and the improvement is evaluated. Using this method, first, optimization of a fibrous filter, similar as discussed by Azimian et al.,[7] is conducted. In a second step, a granular filter, based on the general setup by Kerimov et al.,[9] is optimized to illustrate the broad applicability of the presented approach. It is, however, important to emphasize that these two case studies are intended primarily as illustrations. The main aim of this work is to develop and introduce the general methodology. As this is, to the knowledge of the authors, the first multiscale approach to the design of depth filter media, there are still many simplifications made and various open questions remain. We are aware of this and highlight the corresponding aspects throughout the text as well as in the conclusion at the end.

With this study, we also want to enable the full use of current filter-media manufacturing technologies, from advanced nonwoven manufacturing to 3D printing.[10-14] These technologies allow the creation of precisely-defined graded media, sometimes also referred to as gradient media. However, it mostly remains unclear which spatial gradients are exactly desirable for which application, that is, a rigorous design method is missing. The present work is seen as a contribution to such a general design method.

2 | THEORETICAL BACKGROUND

Traditionally, filtration was described by volume-averaged or continuum equations. This approach has been also described as "macrotheoretic paradigm."[15] However, in recent years, also microscale or PS simulations are widely applied, a research movement termed the "microtheoretic paradigm."[15] As our new method incorporates both strategies, some theoretical background for each of them is provided. Depth filtration on the CS is usually modeled by the mass balance

$$\varepsilon \cdot \frac{\partial c}{\partial t} + q \cdot \frac{\partial c}{\partial z} = -\frac{\partial \sigma}{\partial t}, \tag{1}$$

which is coupled to the kinetic equation of deposition, often spelled out as follows:

$$\frac{\partial \sigma}{\partial t} = \lambda \cdot q \cdot c. \tag{2}$$

In these equations, σ is the specific deposit, that is, the retained particle volume per filter bed volume, ε is the bed porosity, c is the volumetric impurity concentration in the suspension, and q is the superficial velocity of the suspension. λ is denoted as filter coefficient and describes the local filter performance which plays an important role for the presented approach. t and z are the independent variables time and space, respectively. The described approach is widely used in literature and has proven successful for many different instances of depth filtration.[3,4,8] Assuming stationary behavior and a constant filter coefficient λ, Equations (1) and (2) can be simplified to the well-known Iwasaki equation:[16]

$$\frac{dc}{dz} = -\lambda \cdot c. \tag{3}$$

The Iwasaki equation is related to overall filtration efficiency, that is, the overall reduction in impurities while the suspension passes through the filter. Solving Equation (3) by separation of variables leads to

$$c_L = c_0 \cdot \exp\left(-\int_0^L \lambda(z) dz\right) = c_0 \cdot e^{-\bar{\lambda} \cdot L}, \tag{4}$$

where c_0 and c_L are the concentration values at the filter inlet ($z = 0$) and outlet ($z = L$), respectively, and $\bar{\lambda}$ is the mean filter coefficient. As usually λ changes with deposition, it is often expressed in the literature as a function of σ:

$$\lambda = \lambda_0 \cdot F(\sigma, \mathbf{P}), \tag{5}$$

where F is a functional expression that modifies the initial filter coefficient, that is, of the unclogged filter, depending on the deposition and a number of model parameters contained in the parameter vector $\mathbf{P}$.[3,4,8,17] Thus, only for short filtration times, the assumption $\lambda = \lambda_0$ can be made, which also implies $F = 1$. For these times, the local filter coefficient is not yet strongly affected by separated material within the filter. This is exactly the assumption we make in the remaining article.

In contrast to these continuum models, microscale or PS simulations resolve the true multi-phase information of the suspension and the porous material. Flow within the pore space is computed by solving the fluid transport equations, such as the Stokes, Navier–Stokes, or Euler equations. Particles in the suspension are modeled as discrete elements. When simulating depth filtration, models for the interaction of fluid and dispersed particles as well as between particles and the surfaces of the filter material are incorporated.[18,19] Please note that all variables of the discussed continuum equations can be interpreted as volume averages of the microscale behavior.[20-22] Thus, there is an established theoretical framework for the upscaling from microscale or PS to CS.

3 | COMPUTATIONAL STRATEGY

3.1 | Pore-scale simulations

PS simulations are conducted in GeoDict (version: GeoDict 2018 Service Pack 3 Standard Edition, supplier: Math2Market, Kaiserslautern, Germany). Structures for both case studies are created using the GeoDict modules "FiberGeo" and "GrainGeo."[23,24] Fiber or grain overlaps with a voxel length of 1 μm are prohibited or, if necessary, removed automatically by the software. In preliminary studies, a representative domain size was determined for both investigated

cases such that, on the one hand, porosity has converged and all expected effects are captured, but, on the other hand, still reasonable simulation times can be achieved, that is, less than 1 day.

Filtration simulations based on these structures are performed using the module "FilterDict." The mode "Filter Life Time - Single Pass" is chosen together with the left-identity-right (LIR) solver which is based on adaptive grids and allows for comparatively short computation times. This mode uses discrete time steps, called batches, to pass a monodisperse suspension through the filter at a constant flow rate and particle concentration until a maximum filtration time (t_{max}) is reached. As already mentioned, only short filtration times are considered in this work to justify the assumption of an approximately constant filter coefficient. In this respect, the time span of 10 batches was determined in a preliminary simulation study as representative for the short-time behavior for both case studies, that is, the fibrous and the granular media.

For all simulations, the flow field in the pore space is computed based on Stokes law, that is, inertial effects are neglected. This is justified due to the small Reynolds numbers[6] which did not exceed 0.5 in any case. Also, Brownian motion of the suspended particles is included. Electrostatic interaction between particles and surfaces is neglected. Particle capture is modeled by two different modes, as explained when the two case studies are discussed in detail. Deposited impurity particles change the pore space which is considered in the subsequent computation of flow field and particle capture. Reentrainment of separated impurity particles is not modeled. More information on the simulation strategy is found in the software documentation[19,25] as well as in the publications from which we adapted our two case studies.[7,9] A triple determination was conducted for all simulation setups of this article, that is, we used three different random-number seeds for creating the fiber or grain structures, respectively, and conducting the filtration experiments.

3.2 | Fibrous filter media

As the first case study, a fibrous filter medium is considered. This case study is based on the work of Azimian et al.[7] Using the "create" mode of GeoDict's "FiberGeo" module, a bimodal glass fibers packing is created in a domain of 300 × 300 × 600 voxels. Fibers of two different sizes are used. In all considered cases, the coarse fibers are uniformly distributed over the filter height with constant solid volume fraction (SVF) of 3.67%, a diameter of 20 μm, and an anisotropic orientation of 8/1. For more details on the meaning of the last value, the reader is referred to the GeoDict documentation.[19] They serve as a support structure in which the fine fibers, with diameter of 4 μm and also anisotropic orientation of 8/1, are embedded. Their volume fraction, referred to as fine fiber fraction, is varied and also serves as the control variable for the optimization.

Using a total SVF between 5 and 10 vol%, filtration simulations were carried out, consecutively raising the SVF by 0.5 vol%. Figure 1 shows three exemplary fibrous structures with varying fine fiber fraction.

For the filtration simulations, the fluid is oil at a temperature of 20°C, a density of 839.4 kg m^{-3}, and dynamic viscosity of 0.04998 kg m^{-1} s^{-1}. Additionally, an inflow and outflow region of 50 empty voxels each, is added to the structure to ensure proper inflow and outflow behavior, producing a total domain height of 700 voxels. A time step per batch of 10 s per filtration simulation is used and a t_{max} value of 100 s. As already explained, the short filtration time is chosen to prevent significant changes in local separation properties due to deposition, thus supporting the assumption of an approximately constant λ. An impurity concentration of 5×10^{-5} g L^{-1} and a flow rate of 60 L min^{-1} is chosen for the suspension; the filter area is set to 100 cm^2. Impurities are single-sized spherical particles with a diameter of 2 μm and a density of 2,560 kg m^{-3}. Particles are modeled by the "resolved particles empty/solid" mode, as required by GeoDict due to their size being larger than the voxel size. For the separation mode, "caught on first touch" is chosen, that is, sticky particles are assumed that are filtered at the point of first contact. These setting result in a total of 10 batches per simulation and 405 particles per batch. The main differences to the study of Azimian et al.[7] are that single-sized instead of polydisperse particles are used, single-pass instead of multi-pass simulations are carried out, and that the capture mode is "caught on first touch" instead of "sieving."

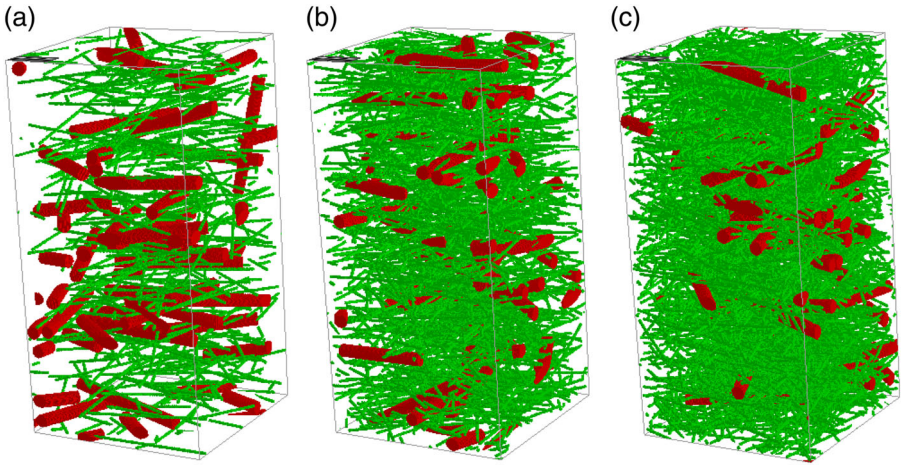

FIGURE 1 Exemplary fibrous media used for determining the continuum-scale parameters. Fine fibers are shown in green and coarse fibers in red; here, both fiber types are homogeneously distributed over the filter height. The solid volume fraction (SVF) of fine fibers is 5.0 (a), 7.5 (b), and 10.0 vol% (c) [Color figure can be viewed at wileyonlinelibrary.com]

In order to validate the optimization approach on the PS, structures with varying composition along their depth are generated, that is, graded fibrous media. Using the option "density distribution" in the module "FiberGeo," the structure can be cut into sections along the z axis and each an individual SVF can be assigned. By this method, the fine fibers are nonhomogeneously distributed as predicted by the continuum models using 10 sections, while the coarse fibers remain unchanged.

3.3 | Granular filter media

A filter medium composed of packed grains is considered in the second case study. This case study is based on the work of Kerimov et al.[9] from which also the main parameters are adapted. The particle packing is composed of spherical particles of two sizes, a small grain diameter D_1 of 15.5 μm and a coarse grain diameter D_2 of 31 μm which results in a diameter ratio of $D_2/D_1 = 2$. Particle packings are generated using GeoDict's GrainGeo module and the "pile" mode. Contrary to the cylindrical domain of Kerimov et al.[9] which accommodated 2,000 particles at a ratio D_{domain}/D_2 of 13 and a height to width ratio of one, a quadratic filter area is chosen here. After piling the 31 μm diameter grains (host particles) into a structure of 400 × 400 × 400 voxels, 2,300 objects were counted. The difference compared to the study of Kerimov et al.[9] is attributed to the different shapes of the simulation domain. The structures for the simulation are piled using a preset between 0 and 50 vol% of the small grain fraction (SGF), starting at 0 vol % and consecutively increasing it by 10%. The volume fraction of coarse grains for all structures was (100—SGF) vol%, respectively. Figure 2 shows three example structures created by this method. Using ratio values such as 50:50, 70:30, and so forth, with the first value representing the vol% coarse grains and the second representing vol% small grains, the structures will also be described.

For the filtration simulations, the fluid is air at a temperature of 20°C, a density of 1.204 kg m^{-3}, and dynamic viscosity of 1.834×10^{-5} kg m^{-1} s^{-1}. Inflow and outflow region heights are chosen to be 56 voxels since the total structural height would equal 512 which as power of two has good computational parallelization properties. An impurity concentration of 3×10^{-5} g L^{-1}, a flow rate of 60 L min^{-1}, and a total filter area of 100 cm^2 is used. The impurities consist of spherical particles with a diameter of 2.325 μm, a constant density of 2,560 kg m^{-3}, and a restitution coefficient of 0.5 which describes the ratio of rebound velocity to impact velocity. Similar to the first case study, the "resolved particles empty/solid" option is chosen to model the particles. However, a different particle capture mode is employed; "sieving" is assumed here as is done by Kerimov et al.,[9] that is, particles are separated only if they are stuck geometrically. Equal to the first case study, a time step per batch of 10 s and a maximal simulation time t_{max} of 100 s is used. This results in 275 particles per batch in the granular-media case study.

The filter inlet and outlet of the grain structures show significant deviations from representative packings due to the spherical shape of the particles and the resulting uneven surfaces. As these deviations significantly impact the deposition behavior, especially at the filter inlet, and, therefore, the λ value determined by model fitting, the simulation data of all granular media are processed for filtration batch. Individually adapted, the first 30–50 voxels of the filter inlet are cut and filter height as well as particles entering per batch are recalculated as described in more detail in the Appendix S1 (available online).

Analogous to the first study, optimization results are validated on the PS. As the module "GrainGeo Pile" does not have the option of creating a particle distribution over height, the structure is created in a step-by-step process. The calculated SGF over height function is divided into 10 equal parts of 40 μm and the average SGF per part is calculated. A 400 × 400 × 40 voxel structure is created and "filled to rim" with the average preset SGF of the first 40 μm. Note that these 40 μm are sufficient to accommodate one layer of coarse grains. Then, 40 empty voxels are added to the height of the structure forming a 400 × 400 × 80 voxel structure and the added voxels are again "filled to rim" with the new SGF averaged from 40 to 80 μm averaged value. The process is repeated until the structures' dimension is 400 × 400 × 400 voxels.

3.4 | Parameter estimation and optimization on continuum scale

We now turn to the CS operations; first, parameter estimation (PE) is discussed, second, optimization is considered. Using the GeoDict module "GeoLab," the files are converted to multidimensional arrays

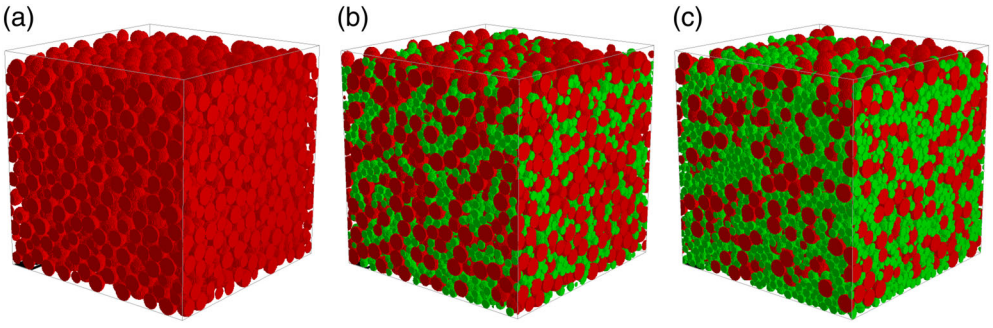

FIGURE 2 Exemplary granular media used for determining the continuum-scale parameters. Fine grains are shown in green, large grains in red; here, both grain types are homogeneously distributed over the filter height. The volumetric ratio of coarse to small grains is 100:0 (a), 70:30 (b), and 50:50 (c) which corresponds to a small grain fraction (SGF) of 0 vol% (a), 30 vol% (b), and 50 vol% (c) [Color figure can be viewed at wileyonlinelibrary.com]

of the same sizes as the corresponding 3D simulation domains and exported to MATLAB (version: R2016a; MathWorks, Natick, MA) where further analysis is conducted. All different phases, that is, filter materials, deposited particles, and pore space, are distinguished by the assigned numbers on the corresponding positions within the arrays. Data on deposited particles are available for each filtration batch, that is, the full time evolution of deposition is accessible. Please note that the granular media are individually cut on the top to avoid artifacts at the inlet, as previously addressed and described in more detail in the Appendix S1.

Using the data on specific deposit as a function of filter depth, the filter coefficient λ in the continuum models is determined by conventional PE. In MATLAB, the least-square problem is approached by the solver "lsqnonlin" with its default settings. The objective function for PE is given by

$$J_{\mathrm{PE}}(\lambda) = \sum_{i=1}^{i=N} \left[\sigma_{\mathrm{PS}}(z_i) - \sigma_{\mathrm{CS}}(z_i\lambda)\right]^2, \tag{6}$$

where σ_{PS} is the specific deposit per unit of filter bed volume extracted from the PS simulations and σ_{CS} is the specific deposit per unit of filter bed volume predicted on the CS. Therefore, in order to determine the filter coefficient λ, the quadratic difference between the deposition profiles is minimized. In this case, the depth coordinate z_i is also discretely given for the N layers of the filter medium, that is, i = 1, 2, ..., N. σ_{PS} is obtained from the PS simulations as described at the beginning of this section. σ_{CS} is calculated from the CS model. It is obtained when separation of variables and integration is applied to Equation (2):

$$\sigma_{\mathrm{CS}}(z) = \lambda \cdot q \cdot c(z) \cdot t^*. \tag{7}$$

Note that the time t^* is considered here as a time span, that is, the duration of filtration, and enters the calculation, therefore, as a parameter, not an independent variable. Inserting Equation (4) into Equation (7) and assuming a constant filter coefficient λ over filter depth, as is the case when the parameter fitting is conducted, yields:

$$\sigma_{\mathrm{CS}}(z) = \lambda \cdot q \cdot c_0 \cdot \exp(-\lambda \cdot z) \cdot t^*. \tag{8}$$

Now, Equation (8) may be simplified further, in order for it to be independent of time and total filtrated volume. Using the basic definitions for superficial velocity

$$q = \frac{\dot{V}}{A} = \frac{V}{t^* \cdot A} \tag{9}$$

and inlet impurity concentration

$$c_0 = \frac{V_p}{V}, \tag{10}$$

the specific deposit may be defined as

$$\sigma_{\mathrm{CS}}(z) = \frac{\lambda V_p}{A} \cdot \exp(-\lambda \cdot z), \tag{11}$$

with A being the filter area, V the total filtrated volume, and V_p the total volume of impurity particles entering the filter. For our two case studies, the dependency of filter coefficient λ on the composition of the filter media is determined, that is, λ is correlated with the volumetric fraction ϕ of the media's constituents (small/large fibers or small/large grains), that is, the following function is fitted to the PS data:

$$\lambda(\phi) = P_1 + P_2\phi + P_3\phi^2. \tag{12}$$

P_1 to P_3 are model parameters. Examples of fits of Equation (12) are shown in the results section.

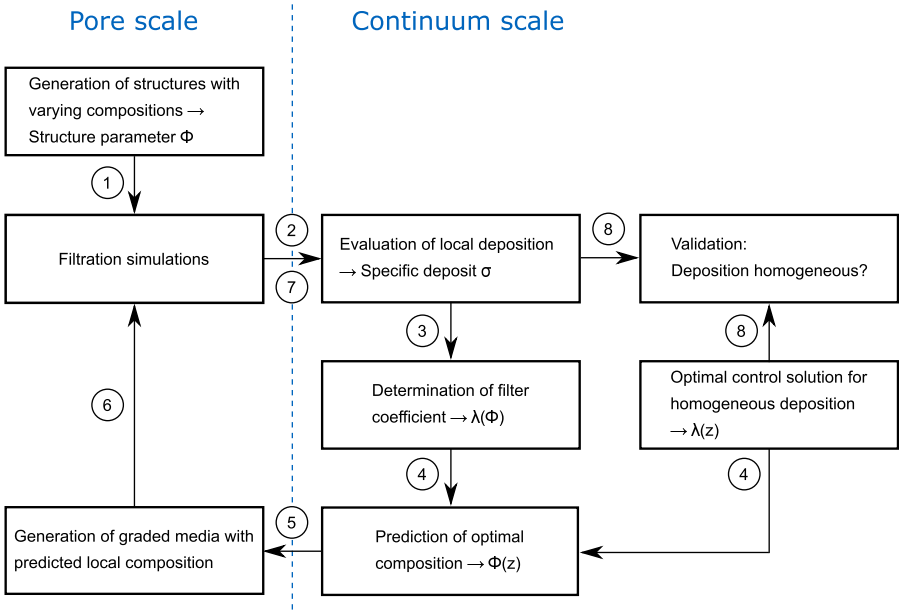

FIGURE 3 Overview over the multiscale optimization approach; the processing order is marked by the circled numbers [Color figure can be viewed at wileyonlinelibrary.com]

Having explained the determination of λ as dependent on the filter's geometry, next, filter-media optimization using the parameterized continuum model is addressed. The objective is to achieve homogeneous deposition within the filter media using filter coefficient λ as the control variable. Following Kuhn et al.,[8] the goal of homogeneous deposition can be formulated using the objective function

$$J_{OC}(\lambda(z)) = \int_0^L [\bar{\sigma} - \sigma(z,\lambda(z))]^2 dz \tag{13}$$

from which, applying Equations (2) and (3), the following trajectory of the filter coefficient can be derived[8,26]:

$$\lambda(z) = -\left[L \cdot \left(\frac{c_0}{\Delta c} + \frac{z}{L}\right)\right]^{-1}. \tag{14}$$

L is filter media's height and known form the microscale simulations. $\Delta c = c_L - c_0$ corresponds to the desired overall reduction in impurities. In this study, a reduction of 80% is considered, that is, $c_L = 0.2 \times c_0$. As a trajectory of λ, that is, $\lambda(z)$ is determined here, the approach is an optimal control method, in contrast to conventional optimization where only point values are determined.[27,28] Therefore, the subscript OC is used in Equation (13) which denotes "optimal control." The whole multiscale approach is again schematically shown in Figure 3. In order to compare the two optimized filter media, that is, graded media, with suitable equivalents, nongraded media with the same filtration efficiency are generated and analyzed. Using Equation (4), the filter coefficient for such a structure is obtained from

$$\lambda = \frac{1}{L} \cdot \ln\left(\frac{c_0}{c_L}\right). \tag{15}$$

4 | RESULTS AND DISCUSSION

As illustrated in Figure 3, the general strategy of the presented multiscale approach is as follows: We use the PS deposition data to establish a correlation on the CS between filter coefficient and geometrical information, that is, composition of fiber or grain packings, respectively. This correlation is subsequently used to optimize the filter media. Following this succession, first, some exemplary deposition results are presented. After that, we address both case studies separately and show the found filter coefficient–geometry correlations for fibrous and granular filter as well as their use for optimizing the two types of filter media.

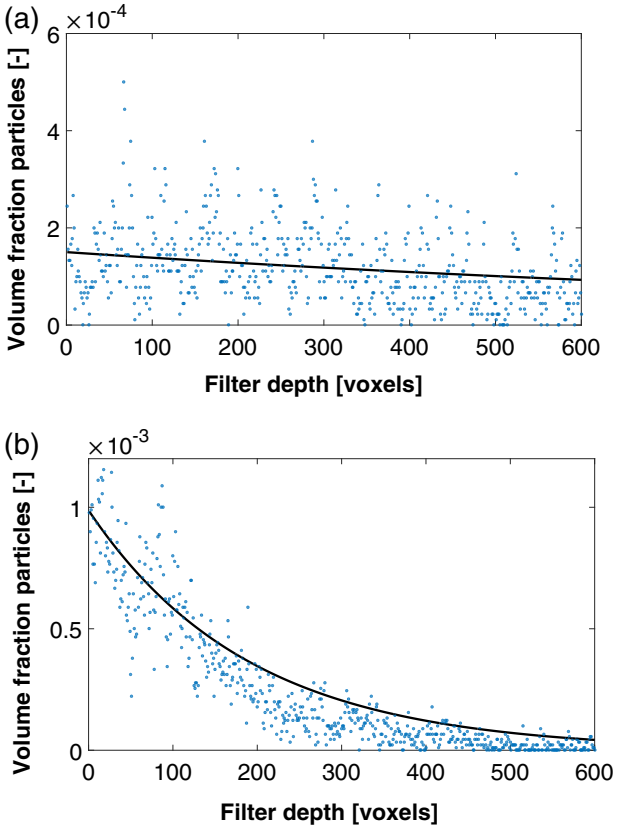

FIGURE 4 Volume fraction of deposited particles for fibrous filter media with a total solid volume fraction (SVF) of 5 vol% (a) and 10 vol % (b); black lines represent curve fits used to determine the filter coefficient [Color figure can be viewed at wileyonlinelibrary.com]

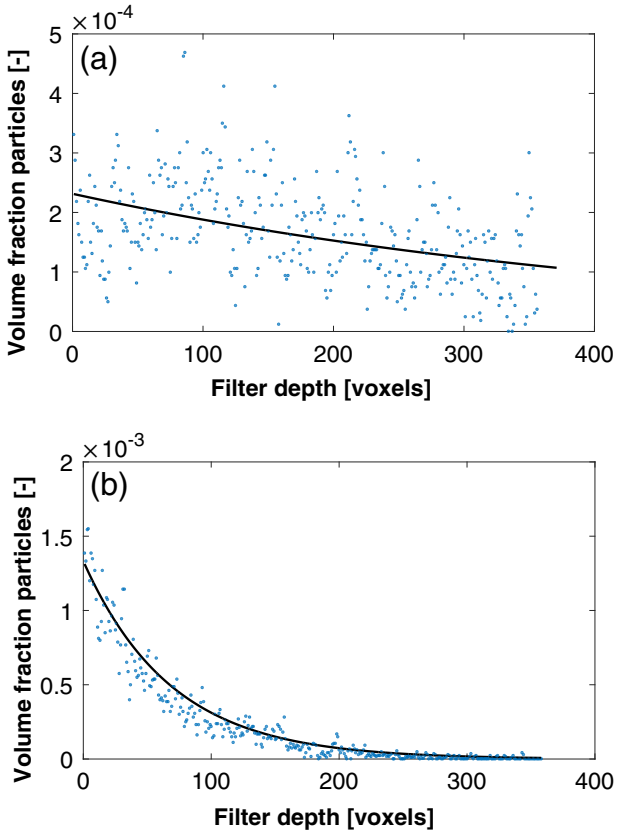

FIGURE 5 Volume fraction of deposited particles for granular filter media with a small grain fraction (SGF) of 0 vol%, i.e., only coarse particles (a), and 50 vol% (b); dashed lines represent curve fits used to determine the filter coefficient [Color figure can be viewed at wileyonlinelibrary.com]

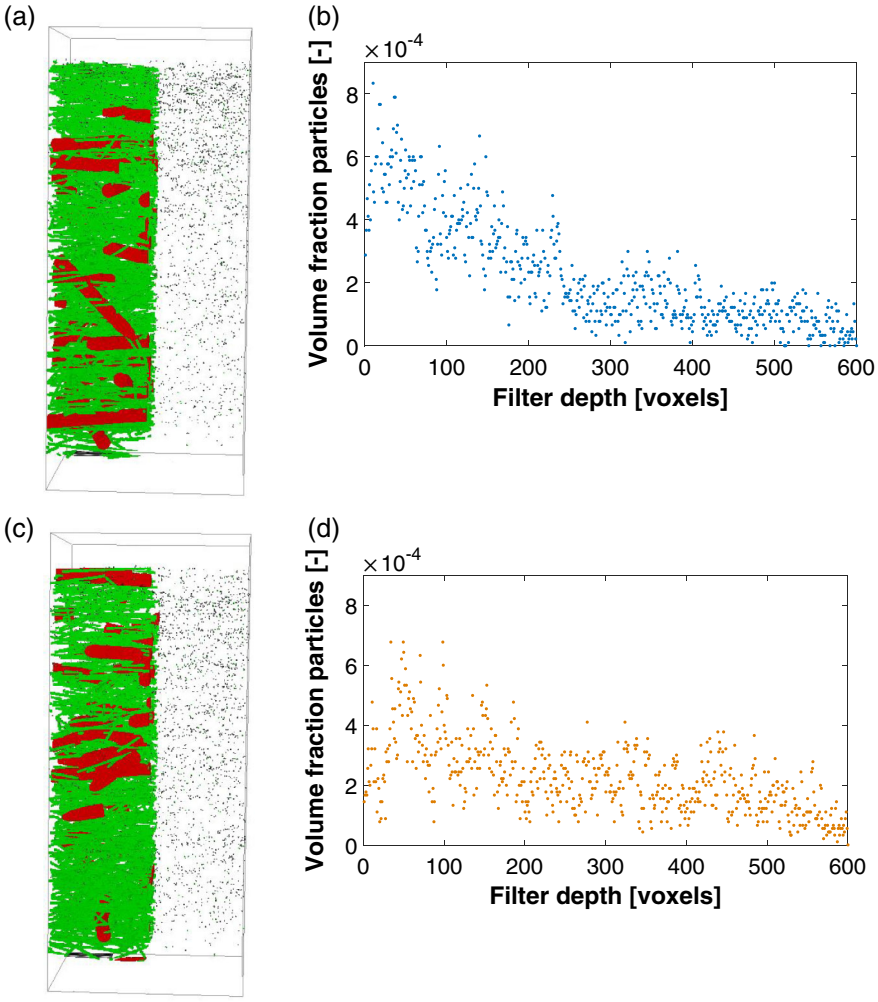

FIGURE 7 Exemplary visualization (a,c) and volumetric evaluation of impurity particles (b,d) after 10 filtration batches for homogeneous, that is, nongraded, reference structure (a,b) and optimized graded fibrous medium (c,d). In the shown filter media (a,c), half the structures are made transparent to display the internally deposited particles (depicted in black). As all three performed simulation runs show a similar behavior, only results of one simulation are shown [Color figure can be viewed at wileyonlinelibrary.com]

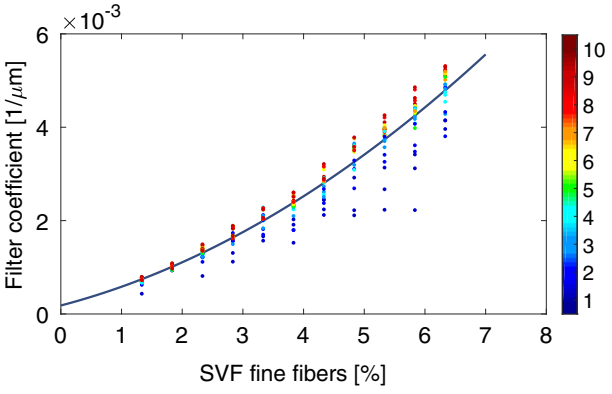

FIGURE 6 Dependence of filter coefficient λ on solid volume fraction (SFV) of fine fibers in case of the fibrous filter media. Relation shown for all investigated filtration batches; the color bar indicates the number of batches, reaching from Batch 1 (dark blue) to Batch 10 (dark red). As all simulation setups were performed three times, points of the same color denote the repetitions of the same batch. The black line shows the fitted function used to correlate the filter media composition (SFV of fine fibers) with the filter coefficient [Color figure can be viewed at wileyonlinelibrary.com]

4.1 | Deposition

It is found that denser structures, that is, with a higher overall SVF, show a larger overall filtration efficiency. They also exhibit a stronger gradient in the local deposition with the highest deposition at the filter inlet. Figure 4 shows exemplary deposition results for fibrous filters with SVF of 5 and 10 vol%, respectively.

Corresponding results for the granular-filter case study are depicted in Figure 5 for SGFs of 0 and 50 vol%. An analogous behavior as shown in Figure 4 for the fibrous media can be observed. Note that the domain cut, as described earlier and in the Appendix S1, has been applied for the granular filters, including the corresponding shift of the coordinate system and the correction of the particle concentration in the suspension. The gradient in local deposition, observed in both case studies, is well known from literature.[29-31] In our case, denser structures, that is, with a higher SVF, also lead to smaller pore sizes and a higher specific surface. This explains the more pronounced hold-up of impurity particles with increasing SVF due to the higher collision probability between impurity particles and filter surfaces.[17,32] All black lines in Figures 4 and 5 correspond to fits of Equation (11).

TABLE 1 *SD* of specific deposit $\sigma(z)$ over depth of fibrous filters shown for the three performed repetitions (Structure #)

Structure # (–)	Homogeneous structure (–)	Optimized structure (–)	Improvement (%)
1	1.765×10^{-4}	1.204×10^{-4}	31.8
2	1.841×10^{-4}	1.128×10^{-4}	38.7
3	1.701×10^{-4}	9.953×10^{-5}	41.5

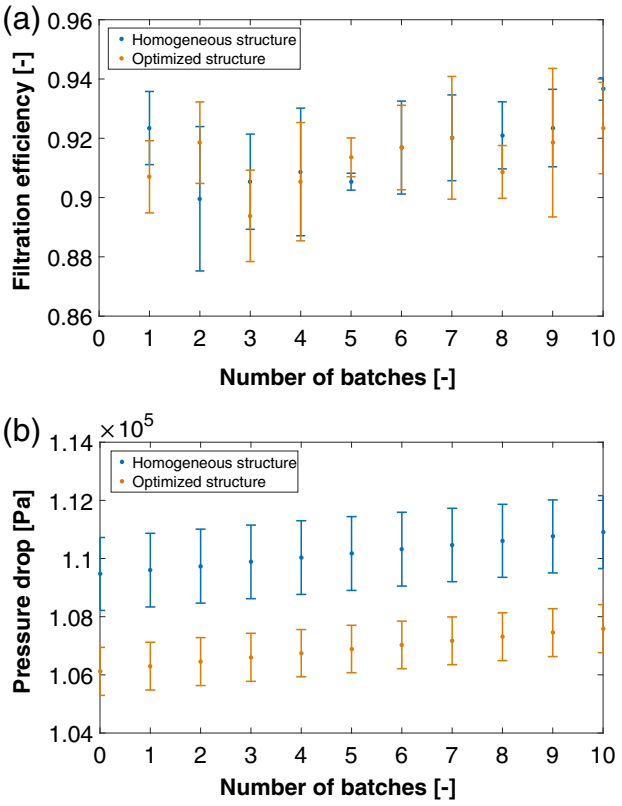

FIGURE 8 Comparison of the filtration efficiency (a) and pressure drop (b) of the optimized, that is, graded (orange), and homogeneous, that is, nongraded, fibrous media (blue). The error bars indicate the *SD* obtained from the three repetitions of all simulation setups [Color figure can be viewed at wileyonlinelibrary.com]

These curve fits are used to determine the filter coefficient λ for the continuum models.

4.2 | Optimization of fibrous media

Using the curve-fit data, a correlation is established between the filter coefficient λ and the composition of the filter media. For the first case study, therefore, different fibrous media are created and analyzed. Figure 6 displays the λ values calculated for each batch and SVF of fine fibers. Here, only fine fibers are considered as the SVF of coarse fibers is kept constant.

In general, Figure 6 confirms the just observed trend that structures with a higher SVF lead to a more efficient separation which

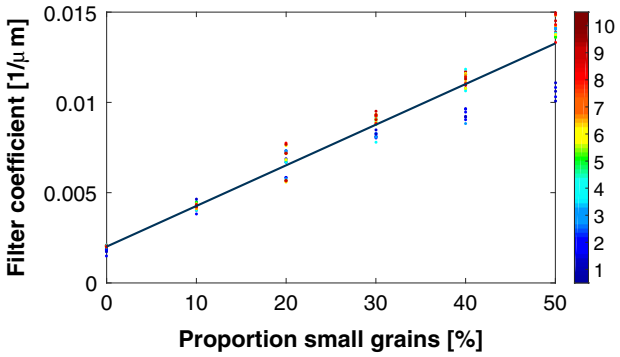

FIGURE 9 Dependence of filter coefficient λ on proportion of small grains, that is, small grain fraction (SGF), in case of the granular filter media. Relation shown for all investigated filtration batches; the color bar indicates the number of batches, reaching from Batch 1 (dark blue) to Batch 10 (dark red). As all simulation setups were performed three times, points of the same color denote the repetitions of the same batch. The black line shows the fitted function used to correlate the filter media composition (SGF) with the filter coefficient [Color figure can be viewed at wileyonlinelibrary.com]

corresponds to a higher value of the filter coefficient λ. This can be explained by a larger specific surface with increasing SVF and, therefore, a higher probability of particle capture. Additionally, it can be seen that λ is not independent of the filtration batch, that is, of how many particles are already deposited within the filter medium. As already explained, deposition changes the filter medium and, therefore, affects further separation behavior. However, as only short times are considered in this study, this effect is not investigated in detail here and only the average behavior over 10 batches is further used. As explained, in this time span, the filter coefficient can be considered approximately constant. The shown data points are fitted to Equation (12). In this first case study, ϕ takes the meaning of SVF of fine fibers. Fitting leads to values of $P_1 = 1.817 \times 10^{-4}$ μm^{-1}, $P_2 = 3.406 \times 10^{-4}$ μm^{-1}, and $P_3 = 6.111 \times 10^{-5}$ μm^{-1}. Equating this correlation with the optimal trajectory of the filter coefficient $\lambda(z)$ as presented in Equation (14) and resolving the quadratic equation for $\phi(z)$ yields:

$$\phi(z) = \frac{-P_2 + \sqrt{P_2^2 - 4 \cdot P_3 \cdot (P_1 - \lambda(z))}}{2 \cdot P_3}. \tag{16}$$

Using the results of Equation (16), a graded fibrous structure is generated in GeoDict using 10 equally thick slices in the depth direction of the filter medium. For comparison, a nongraded, that is, homogenous, structure with the same overall filtration efficiency is created relying on the prediction of Equation (15) and translating the obtained λ value again into a corresponding filter medium composition applying Equation (16). For $c_0/c_L = 5$ and a filter depth $L = 600$, a λ value for the homogeneous structure of 0.0026824 μm^{-1} is calculated which corresponds to SVF of fine fibers of 4.1909 vol%.

First, it is checked how well the optimization goal, as formulated in Equation (13), is reached. Figure 7 shows the volume fraction of deposited particles in the homogenous and the optimized fibrous

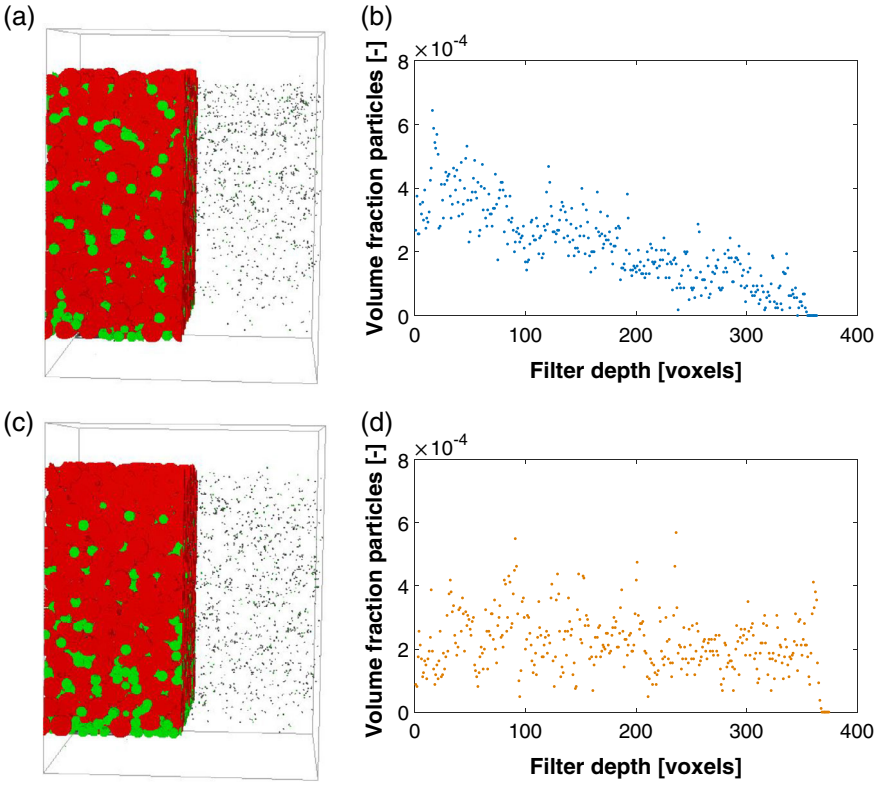

FIGURE 10 Exemplary visualization (a,c) and volumetric evaluation of impurity particles (b,d) after 10 filtration batches for homogeneous, that is, nongraded, reference structure (a,b) and optimized graded granular medium (c,d). In the shown filter media (a,c), half the structures are made transparent to display the internally deposited particles (depicted in black). As all three performed simulation runs show a similar behavior, only results of one simulation are shown [Color figure can be viewed at wileyonlinelibrary.com]

structure. One filtration run is presented as an example, the other two repetitions exhibit the same qualitative behavior. Already by visual inspection, it is seen that the optimized graded structure (Subfigures c and d) shows a much more homogenous deposition profile compared to the nongraded medium (Subfigures a and b). With respect to Figure 7, it is important to note that the results are displayed as usual in depth filtration studies: When structures are shown (as in Subfigures a and c), flow direction is vertical and the suspension enters at the upper end of the filter; in contrast, specific deposit is plotted on the y axis over filter depth shown on the x axis (in Subfigures b and d). Therefore, Subfigures a and b illustrate the same behavior, namely, the more pronounced deposition of impurity particles at the filter inlet. The same conventions of display are used again in Figure 10.

In order to quantify this behavior, the standard deviation (*SD*) of local deposition for all three filtration runs are shown in Table 1. The homogeneity, as measured by the *SD*, improved in all cases and increased on average by 37.3%.

In addition to the optimization goal, also the overall filtration efficiency and pressure drop of the homogeneous and the optimized graded media are compared. Figure 8 shows the corresponding results as they change over filtration time, that is, over the conducted batches.

The average filtration efficiency of the homogeneous and optimized structure are 91.605 and 91.259%, respectively. Since a filtration efficiency of 80% was aimed at, an increase of roughly 11% can be noticed for both the homogenous and the optimized graded structure. Furthermore, no significant trend following the number of batches is found. It is, therefore, conjectured that the upscale-downscale procedure still contains some uncertainties in case of the investigated fibrous media. Nevertheless, the agreement is still fair, considering the loss of details when upscaling from the PS to the CS.

The overall pressure drop difference between the homogeneous and optimized structure differs around 0.03–0.04 $\times 10^5$ Pa, therefore, the optimized medium leads to lower pressure drops. Batch 0, depicts the pressure drop prior to the first batch, and does not show a significant deviation from the trend for both structures. Starting at Batch 1 with a pressure drop of 1.0947 $\times 10^5$ Pa and 1.0612 $\times 10^5$ Pa, a linear increase to 1.1091 $\times 10^5$ Pa and 1.0759 $\times 10^5$ Pa can be observed for the homogeneous and optimized structure, respectively. Thus, no significant difference in the increase of total pressure drop, 0.01308 $\times 10^5$ Pa for the homogeneous and 0.01290 $\times 10^5$ Pa for the optimized medium, is observed. However, as filtration time increases, the gradient is expected to differ, similar to the graded fibrous media simulated by Azimian et al.[7] Please note that the optimized graded media lead to a lower pressure drop even though the overall SVF of the nongraded fibrous media (7.86%) is very similar to the optimized media (7.7195%).

4.3 | Optimization of granular media

An analogous succession as for the fibrous media is now presented for the granular-media case study. λ values determined by fitting of Equation (11) to the deposition results based on grain structures with varying composition are displayed in Figure 9. As the SGF increases, the filter coefficient λ grows due to the smaller pores created and the thus higher probability of particle capture. Also the spread of λ values

TABLE 2 *SD* of specific deposit $\sigma(z)$ over depth of granular filters shown for the three performed repetitions (Structure #)

Structure # (–)	Homogeneous structure (–)	Optimized structure (–)	Improvement (%)
1	1.255×10^{-4}	9.341×10^{-5}	25.6
2	1.237×10^{-4}	8.750×10^{-5}	29.3
3	1.366×10^{-4}	8.923×10^{-5}	34.7

grows with raising SGF. Similar to the fibrous media, the increasing spread can be explained by the more pronounced separation of impurity particles in denser filter media and the stronger change of these media caused by the deposited particles.

Due to the nature of the data shown in Figure 9, P_3 in Equation (12) is set to zero, that is, a linear curve is fitted. With L = 400, the coefficients are $P_1 = 2.013 \times 10^{-3}$ μm^{-1} and $P_2 = 2.251 \times 10^{-4}$ μm^{-1}. Combining the resulting linear equation with the optimal control solution of Equation (14) and resolving it for $\phi(z)$ yields:

$$\phi(z) = \frac{\lambda(z) - P_1}{P_2}, \tag{17}$$

where ϕ represents the SGF. The $\bar{\lambda}$ for the homogeneous, that is, nongraded, structure, with c_0/c_L = 5 and L = 400 according to Equation (15) is determined as 0.0040236 μm^{-1}. Recalculating the SGF with the linear fit of Equation (17) yields a preset SGF of 8.932%, almost equal to the total preset SGF of the optimized structure.

As for the fibrous media, in a first step the achievement of the optimization goal is checked. The volume fraction of deposited particles in a homogenous and optimized grain structure is depicted exemplarily for one filtration run in Figure 10. Visually, the optimization goal is well met again which is also confirmed by the numerical evaluation presented in Table 2. On the average, the homogeneity of deposition, as quantified by the *SD*, improved by 29.7%.

Figure 11a,b displays the filter-efficiency and pressure-drop results. The optimized structure (orange) has a total average filter efficiency of 81.4% while the homogeneous structure (blue) has 81.8%. As 80% efficiency was aimed-at, the results for the homogeneous structure are only slightly higher than expected and confirm a successful prediction in this case. The average values of filtration efficiency for optimized and homogeneous media do not show significant differences form each other, nor do they exhibit a specific trend with increasing number of batches. Also the overall porosity of the nongraded granular media (42.31%) is very similar to the optimized graded media (42.13%).

The pressure drop of the clean structures, that is, without any deposited particles (Batch 0), is significantly lower than after the first batch (Batch 1) for the homogenous as well as for the optimized media. This behavior differs from the fibrous media as shown in Figure 8. Said difference can be attributed mainly to the different modes of particle capture. Whereas in case of the fibrous media, "caught on first touch" was assumed, sieving is simulated for the granular media. In the mode of sieving, particles are captured only if they have

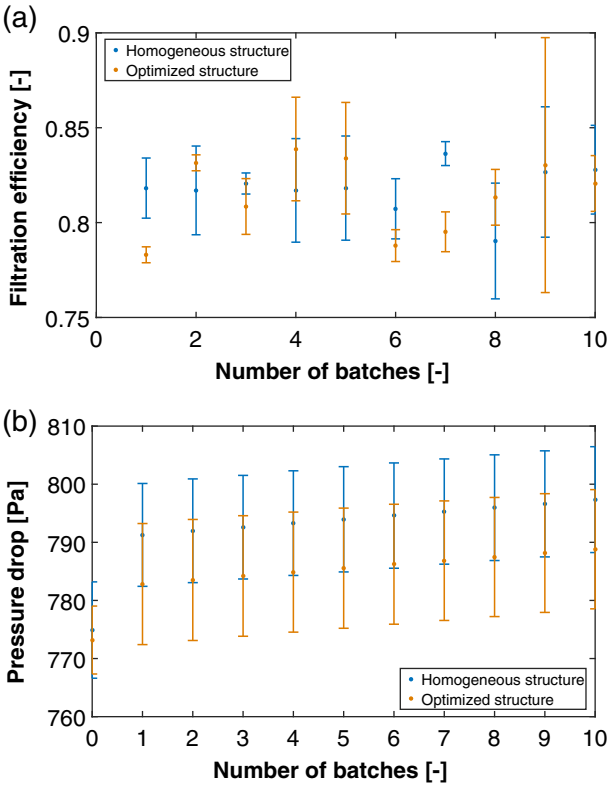

FIGURE 11 Comparison of the filtration efficiency (a) and pressure drop (b) of the optimized, that is, graded (orange), and homogeneous, that is, nongraded, granular media (blue). The error bars indicate the *SD* obtained from the three repetitions of all simulation setups [Color figure can be viewed at wileyonlinelibrary.com]

reached a geometrically stable position in local restrictions. Therefore, suspended particles first clog small-enough pores that offer such restrictions, of which there are also more in case of the more densely packed granular media compared to the open-porous fibrous filters. This initial complete blocking of some pores has a strong influence on the pressure drop as some flow paths are no longer available; however, further capture of particles at the same locations does not affect the pressure drop as much because the corresponding pores are already blocked. The further increase in differential pressure is, therefore, more uniform. For the observed filtration runs, that is, Batches 1–10, the slope of the pressure-drop curves for the homogeneous reference structures as well as for the optimized media is similar. This corresponds to the behavior already observed for the fibrous media.

5 | CONCLUSION

Multiscale approaches are known to be beneficial for various problems. This study shows the first application of a multiscale optimization approach for depth filter media. Not only the microscale data were used for optimizations on the CS, but the predictions from the CS were also validated by microscale simulations. The filter coefficient, quantifying local filtration performance on the CS, was

determined from microscale simulations by a model fit. This was done for various compositions of the filter medium's microscale. Filter coefficient and filter-medium properties were subsequently correlated. Using these correlations, local gradients in medium composition were predicted with the goal to achieve a homogenous deposition of impurities over the depth of the media. These optimized media were compared to structures with approximately the same overall filtration efficiency, but without a gradient in composition.

Two case studies were considered in detail. In each case study, the filter medium was composed of bimodal constituents, fibers of two sizes in the first case, grains of two sizes in the second case. For the fibrous filter, the fluid was oil and the particle-capture mode was "caught on first touch." In case of the granular filter, particles were suspended in air flow and separated by pure sieving. For both case studies, the described multiscale optimization strategy was successful, that is, the homogeneity of deposition within the media could be significantly increased. Therefore, we could show that the local inhomogeneity of impurity deposition encountered in classical depth filters can be eliminated by using media with a spatially inhomogeneous composition, usually referred to as graded media or gradient media. Compared to the nongraded media with similar filtration efficiency, all optimized media also exhibited a lower overall pressure drop. Being successful even though used for different setups, that is, different types of filter media, different fluids, different particle-captures modes, underlines the general validity of the method. And such was the aim of the present article: to introduce the general method.

However, as only the basic strategy was investigated in this article, there still remain various open tasks and interesting research questions. On the PS, it is interesting how different flow conditions and particle-capture modes influence the obtained deposit profiles and, therefore, our multiscale strategy. It is, however, not to be expected that the method as such fails under different PS conditions, but rather that the correlation functions used for the bridging of scales might change. Whereas for validating if our optimization goal, that is, homogeneous deposition, was reached, the evaluation on the CS was sufficient, also the influence of deposited particles on the micro structure, for example, the local pore size distribution, would be interesting. The method so far is only valid for short filtration times, that is, as long as deposition does not yet influence further separation significantly. In order to include changes of the filter coefficient due to deposition, the full problem including Equation (5) needs to be addressed for which, however, the analytical optimal-control solution of Equation (14) is no longer valid. Therefore, the full optimal control problem needs to be solved numerically.[8,26] Furthermore, only monodisperse suspensions were considered in this work. In order to account for polydispersity, it is possible to include different filter coefficients for different size classes of impurities[33] which can be also formulated as a complete population balance model.[34] Often also cake formation on top of depth filters is observed,[7] an effect neglected in the present article. Future work could address this issue by fitting an advanced model on the CS.[35] Also the optimization goal could be changed. We here focused on homogeneous deposition within the filter media because inhomogeneous clogging is a shortcoming repeatedly mentioned in the literature. However, one could also directly maximize achievable filtration times, that is, the times until some maximum pressure drop is reached.[8] Alternatively, overall pressure drop could be kept constant and filtration efficiency could be optimized by locally varying the filter coefficient.

ORCID

Andreas Wiegmann https://orcid.org/0000-0001-5559-8036
Michael Kuhn https://orcid.org/0000-0002-9226-1480

REFERENCES

1. Burganos V, Paraskeva C, Payatakes A. Three-dimensional trajectory analysis and network simulation of deep bed filtration. *J Colloid Interface Sci*. 1992;148(1):167-181.
2. Shanshan M, Ma S, Zhang M, Yang B, Song S, Nie J, Lu P. Preparation of cellulosic air filters with controllable pore structures via organic solvent-based freeze casting: the key role of fiber dispersion and pore size. *BioResources*. 2018.13:5894-5908.
3. Herzig J, LeClerc D, LeGoff P. Flow of suspensions through porous media—application to deep fltration. *Ind Eng Chem*. 1970;62(5):8-35.
4. Zamani A, Maini B. Flow of dispersed particles through porous media—deep bed filtration. *J Petrol Sci Eng*. 2009;69(1–2):71-88.
5. Tien C. *Principles of Filtration*. Amsterdam: Elsevier; 2012.
6. Bear J. Modeling phenomena of flow and transport in porous media. *Theory and Applications of Transport in Porous Media*. Vol 31. Cham: Springer; 2018.
7. Azimian M, Kühnle C, Wiegmann A. Design and optimization of fibrous filter media using lifetime multipass simulations. *Chem Eng Technol*. 2018;41(5):928-935.
8. Kuhn M, Kirse C, Briesen H. Improving the design of depth filters: a model-based method using optimal control theory. *AIChE J*. 2018;64(1):68-76.
9. Kerimov A, Mavko G, Mukerji T, Al Ibrahim M. Mechanical trapping of particles in granular media. *Phys Rev E*. 2018;97(2–1):022907.
10. Kimberly-Clark. Nonwoven filter media market in north america. *Filtr Separ*. 2003;40(9):24-25.
11. Fee C, Nawada S, Dimartino S. 3D printed porous media columns with fine control of column packing morphology. *J Chromatogr A*. 2014;1333:18-24.
12. Ge R, Ghadiri M, Bonakdar T, Hapgood K. 3D printed agglomerates for granule breakage tests. *Powder Technol*. 2017;306:103-112.
13. Low ZX, Chua YT, Ray B, Mattia D, Metcalfe I, Patterson D. Perspective on 3D printing of separation membranes and comparison to related unconventional fabrication techniques. *J Membr Sci*. 2017;523:596-613.
14. Nawada S, Dimartino S, Fee C. Dispersion behavior of 3d-printed columns with homogeneous microstructures comprising differing element shapes. *Chem Eng Sci*. 2017;164:90-98.
15. Kuhn M, Pietsch W, Briesen H. Clarifying thoughts about the clarification of liquids—filtration and the philosophy of science. *Chem Ing Tech*. 2017;89(9):1126-1132.
16. Iwasaki T. Some notes on sand filtration. *J Am Water Works Ass*. 1937;29:1591-1602.
17. Tien C, Payatakes A. Advances in deep bed filtration. *AIChE J*. 1979;25(5):737-759.
18. Mirabolghasemi M, Prodanović M, DiCarlo D, Jikuh H. Prediction of empirical properties using direct pore-scale simulation of straining

through 3D microtomography images of porous media. *J Hydrol*. 2015;529(Part 3):768-778.
19. Planas B, Becker J. *FilterDict-Media/Element2017: User Guide*. Kaiserslautern, Germany: Math2Market; 2017.
20. Gray W. Macroscale equilibrium conditions for two-phase flow in porous media. *Int J Multiph Flow*. 2000;26(3):467-501.
21. Civan F. *Porous media transport phenomena*. Hoboken, NJ: Wiley; 2011.
22. Whitaker S. The method of volume averaging. *Theory and Applications of Transport in Porous Media*. Vol 13. Dordrecht: Springer; 1999.
23. Planas B. *FiberGeo 2017: User Guide*. Kaiserslautern, Germany: Math2Market; 2017.
24. Planas B. *GrainGeo 2017: User Guide*. Kaiserslautern, Germany: Math2Market; 2017.
25. Planas B, Linden S. *FlowDict 2017: User Guide*. Kaiserslautern, Germany: Math2Market; 2017.
26. Kuhn M. New Paths in Filtration—Optimal Control Approaches Based on Continuum Models [Ph.D. thesis]. Munich, Germany: Technical Universtiy of Munich; 2018.
27. Sargent R. Optimal control. *J Comput Appl Math*. 2000;124(2000): 361-371. Numerical Analysis 2000. Vol. IV: Optimization and Nonlinear Equations.
28. Kirk D. *Optimal Control Theory*. Mineola: Dover; 2004.
29. Bai R, Tien C. Transient behavior of particle deposition in granular media under various surface interactions. *Colloids Surf A*. 2000;165 (1–3):95-114.
30. Burganos V, Skouras E, Paraskeva C, Payatakes A. Simulation of the dynamics of depth filtration of nonBrownian particles. *AIChE J*. 2001; 47(4):880-894.
31. Yoon J, Germaine J, Culligan P. Visualization of particle behavior within a porous medium: mechanisms for particle filtration and retardation during downward transport. *Water Resour Res*. 2006;42(6). https://agupubs.onlinelibrary.wiley.com/doi/full/10.1029/2004WR003660
32. Civan F. Modified formulations of particle deposition and removal kinetics in saturated porous media. *Transp Porous Media*. 2015;111(2): 381-410.
33. Tien C, Ramarao B. Granular filtration of aerosols and hydrosols. *Butterworths Series in Chemical Engineering*. 2nd ed. Amsterdam: Elsevier; 2007.
34. Yuan H, You Z, Shapiro A, Bedrikovetsky P. Improved population balance model for straining-dominant deep bed filtration using network calculations. *Chem Eng J*. 2013;226:227-237.
35. Iliev O, Kirsch R, Osterroth S. Combined depth and cake filtration model coupled with flow simulation for flat and pleated filters. *Chem Eng Technol*. 2018;41(1):70-78.

SUPPORTING INFORMATION

Additional supporting information may be found online in the Supporting Information section at the end of this article.

How to cite this article: Geerling C, Azimian M, Wiegmann A, Briesen H, Kuhn M. Designing optimally-graded depth filter media using a novel multiscale method. *AIChE J*. 2020;66: e16808. https://doi.org/10.1002/aic.16808